QUANTITATIVE AND QUALITATIVE CHARACTERIZATION OF THE GRANULOMETRY OF AN INCEPTISOL

Janaina Schadosin[a,] , **Sérgio Costa Saab**[b,*,] , **André Maurício Brinatti**[b] and **Luiz Fernando Pires**[b]

[a]Universidade Estadual de Ponta Grossa, 84030-900 Ponta Grossa – PR, Brasil
[b]Departamento de Física, Universidade Estadual de Ponta Grossa, 84030-900 Ponta Grossa – PR, Brasil

Artigo

Granulometry is an initial factor to be considered in soil research as it plays a fundamental role in physical and chemical properties. The objective of this study was to characterize the granulometric fractions of soil, obtained using the screening and sedimentation method. The Dynamic Light Scattering (DLS), Mid-Infrared (MIR), and Scanning Electron Microscopy with Field Emission Gun (SEM-FEG) techniques were used for this purpose. The quantitative results showed that this soil presents high percentage of clay, followed by fine sand fraction, silt fraction and, finally, the coarse sand fraction. The results obtained by DLS qualify this technique as a procedure to evaluate the quality of the granulometric fractionation of the clay fraction. The MIR analyzes detected characteristic vibrational states of minerals such as kaolinite, halloysite, gibbsite, and quartz. Few works in the literature characterize the clay fraction of the soil without chemical treatment using the SEM-FEG technique. Thus, in this work, pseudo-hexagonal structures were identified, typical of the kaolinite mineral and, to a lesser extent, structures with a filamentous needle-like morphology, which can be ascribed to illite and/or halloysite, whose inorganic functional groups were identified by MIR in the clay fraction of the soil.

Keywords: fractionation; clay; DLS; MEV-FEG; MIR.

INTRODUCTION

In soil laboratories, granulometry quantification is one of the initial experiments carried out to obtain textural classes, which play a fundamental role in the soil physical and chemical properties such as density, porosity, water and air flow, and chemical composition.[1] The procedure used includes the use of physical and chemical energy to break the soil aggregates and separate the mineral particles.[2]

However, in many situations the complete separation is hard to achieve due to contamination between different particle sizes resulting from mistaken parameter considerations when calculating the sedimentation time. Dynamic Light Scattering (DLS), which is an accurate, easily reproducible, and fast technique,[3-7] can be considered as an alternative in the qualification and soil physical fractionation procedure. This technique enables particle size calculation based on the light scattering pattern generated in the light interaction with particles dispersed in the sample.[8]

Another difficulty found in granulometry quantification, refers to the soil characteristics related to each fraction aggregate bonds. These bonds can be so strong that chemical and physical procedures cannot break them; therefore, micrography is a great ally in fraction morphology evaluations. Each group of minerals, due to their chemical and physical characteristics, and differentiated crystalline structure, tend to present different morphologies or crystalline behavior.[9]

Although the literature shows several reports[10-14] confirming the Scanning Electron Microscopy (SEM) as a fast and efficient technique to evaluate the morphology of these minerals, it is still difficult to find images evidencing the natural morphology, that is, images obtained from soils without chemical treatment or that have not been subjected to separation and purification processes.

The Infrared absorption spectroscopy technique is considered relatively simple and non-destructive, with the ability to predict different chemical properties of a given material in a single spectrum. Thus, this technique has been commonly used in the mineral and organic characterization of soil grain size fractions.[15-20] In this study, we employ mid-infrared spectroscopy (MIR-Infrared), which uses the 400-4000 cm^{-1} region to study clay minerals and other soil components.[9,16]

This study aimed to characterize the granulometric fractions of a soil, obtained using the physical fractionation method, which consists in screening to obtain the sand fraction and sedimentation for the clay and silt fractions characterization. To evaluate the reliability of the clay fraction separation, this study presents the dynamic light scattering technique as an efficient and practical alternative. At the same time, the infrared technique was used to determine the organic and inorganic groups found in the minerals and the amorphous material found in the soil and in its individual fractions. Finally, SEM-FEG micrography presented the morphology of the minerals found in the clay fraction.

EXPERIMENTAL

Sampling

The samples were obtained from a family farm (25º 28' 0.66" S latitude, 50º 54' 14.13" O longitude and 821 m altitude), in the municipality of Irati, Paraná, Brazil. The soil is used for grazing (free of intense animal trampling) and was classified according to Santos[7] as a "*Cambissolo Háplico Alumínico*" (or according to Soil Taxonomy *Inceptisol*). The soil in that region is mainly composed of primary (muscovite, quartz, and feldspar) and secondary minerals (kaolinite, illite, iron oxides, and gibbsite).[21]

The samples were collected manually in December 2014 and January 2015, from the 0-10 cm and 10-20 cm layers, which are described in this report as surface and depth, respectively. Four disturbed soil samplings were carried out in each layer.[21] The samples were dried in oven at 40 ºC, fractioned, ground and screened in a 2 mm mesh sieve to obtain the air-dried fine earth fraction (ADFE).[2]

*e-mail: scsaab@uepg.br

Physical Fractionation

The physical fractionation was carried out aiming to separate each granulometric fraction of the soil: coarse sand (53-2000 µm), fine sand (20-53 µm), silt (2-20 µm) and clay (0-2 µm).[22]

This procedure was based on the methodology proposed by De Almeida[2] and Christensen[23] employing ultracentrifuge to speed the clay fraction separation process.[24] The methodology used in this study to separate the granulometric fractions is presented below (Figure 1).

The separation procedure is based on the Stokes law, which allows the determination of the sedimentation time of a specific particle of a certain diameter and located at a certain height inside a liquid.[24] The mean density of the soil studied was obtained using the Pycnometer method.[25]

At the end of the procedure, all samples were dried in oven at 40 °C. The mass of each fraction was obtained using analytical scales.

Characterization

Particle Size Analysis using Dynamic Light Scattering

DLS is a technique based on the Brownian motion of particles concept, in which the shock between molecules in a fluid provokes random movement of particles. Such movement makes the light beam to disperse and vary with time.[26] This light dispersion variation over time creates dispersion patterns, which theoretically, considering a single spherical particle, would form light and dark concentric bands that reduce intensity when the radial position increases.[8] While this particle moves, dispersion patterns are recorded, and a diffusion coefficient (D) is calculated. Thus, knowing the medium temperature

and viscosity, the equipment software calculates the particle sizes using the Stokes - Einstein equation:

$$r_h = \frac{k_B T}{6\pi\eta D} \tag{1}$$

where r_h is the particle hydrodynamic radius; k_B is the Boltzmann constant (1.38×10^{-23} J K^{-1}); T is the medium temperature; η is the medium viscosity; and D is the diffusion coefficient.[27]

It seems relevant to emphasize that mathematical algorithms used by the DLS equipment software rely on more complex parameters combined with the Stokes-Einstein equation.[25] The definition presented above briefly and simply outlines the physical concept that underlies the DLS technique.

The DLS analysis to obtain the clay particle size was carried out using a 10 µL supernatant portion from each suspension containing clay mixed with 50 mL distilled water. This solution remained in ultrasound bath for 20 minutes, so that the clay particle dispersion occurred. Next, the solution was placed in plastic cuvettes and analyzed using the equipment Zetasizer Nano ZS90, Malvern brand, with a 90-degree scattering angle.

After the measurements, the mean diameter of the particles contained in the suspension and a graph with the particle size Gaussian distribution and their respective percentages were obtained.

Mid-Infrared Spectroscopy (MIR)

We used around 1-2 mg ADFE, clay, silt and sand samples (a mixture of fine and coarse sand), from both the surface (A) and depth (P). The samples were homogenized with 100 mg dry KBr,
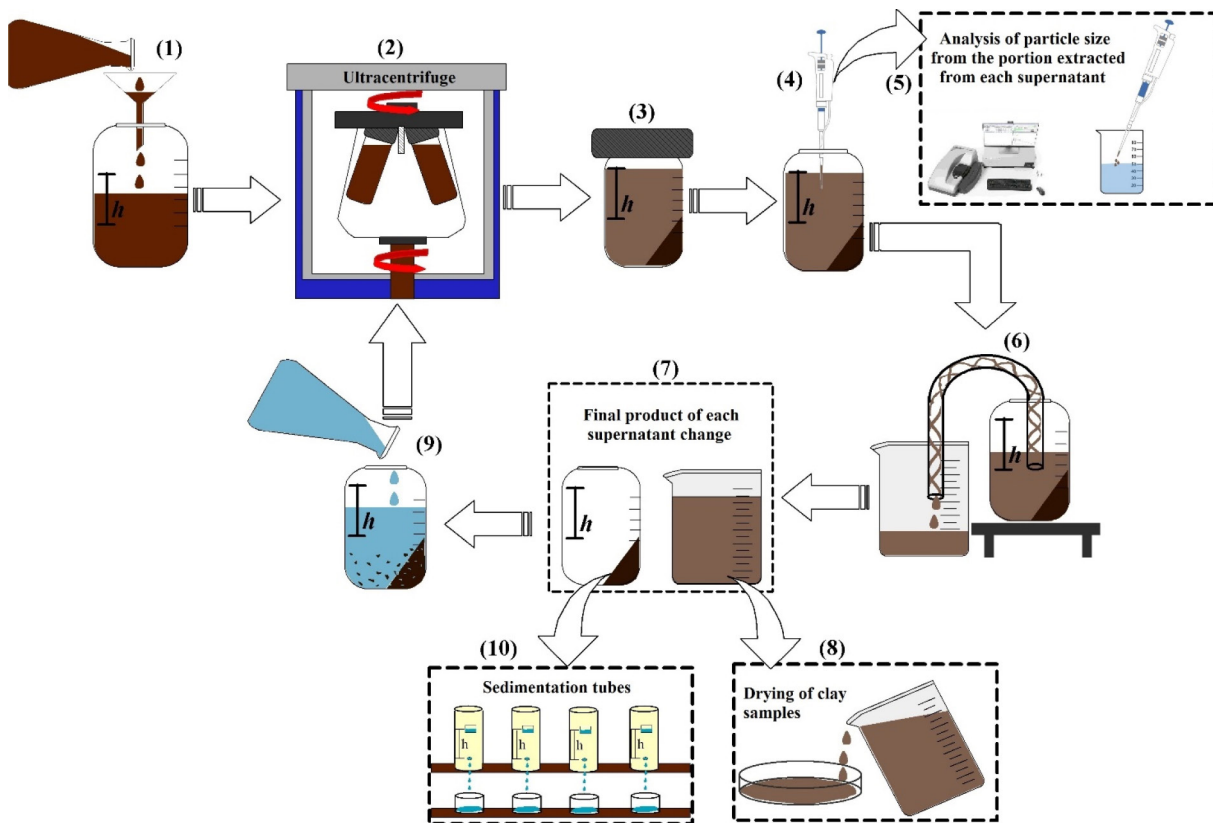
Figure 1. *Soil physical fractionation methodology: (1) The suspension containing fine clay, silt and sand is placed in tubes for centrifugation; (2) Ultracentrifugation is carried out; (3) Precipitation of larger particles (silt, fine sand) occurs with supernatant containing clay in suspension; (4) the supernatant portion is removed; (5) Supernatant DLS analysis is carried out; (6) Supernatant is removed using siphoning; (7) Final product is obtained; (8) The solution containing clay is dried; (9) Resuspension of the precipitate is carried out, aiming to remove any trace of clay (the process is carried out 6 times to secure maximum removal of the clay fraction from the other fractions); (10) The precipitate is fractioned (silt and fine sand) using sedimentation tubes*

in mortar and pestle. The mixture was used to produce pellets under 80 kN/1 cm³ pressure for 5 minutes. A pure 100 mg KBr pellet was produced to obtain the blank. The spectra were obtained with 64 scans, in the 4000-400 cm⁻¹ interval, with a 4 cm⁻¹ resolution in a spectrophotometer of the Shimadzu brand, IRPrestige-21 model.

Scan Electron Microscopy with Field Emission Gun

The clay fraction samples (surface and depth) were homogenized in mortar and pestle and placed on a proper support for microscopy. A carbon band coupled to the support was used to increase the material fixation. The samples were covered in gold using the Shimadzu IC-50 equipment, for 2 minutes at 2 mA and subjected to SEM-FEG by Tescan, Vega 3 model, at 15 kV.

RESULTS AND DISCUSSION

Physical Fractionation

The percentage values of the granulometric fraction contents obtained using physical fractionation by screening and sedimentation are shown below (Table 1).

Table 1. Clay, silt, and sand content

Fraction	Surface (%)	Depth (%)
Clay	51 ± 6	53 ± 4
Silt	18 ± 3	17 ± 2
Fine sand	23 ± 3	23 ± 2
Coarse sand	8 ± 1	7 ± 1

Surface: 0-10 cm layer. Depth: 10-20 cm layer.

These values revealed that the soil presented a clay structure, without significant difference in the granulometric characteristics related to the sample origin (surface or depth). On average, the clay fraction predominated in both the surface and depth, followed by fine sand, silt, and finally, coarse sand. The slight increase in clay content in the deeper layers might be related to the characteristics of the soil origin area. According to Silva,[28] in grazing areas, the soil protection is lower, which might lead to an increase in clay contents in the soil deeper layers.

Characterization

Dynamic Light Scattering Analysis

The use of DLS is reported in the literature as a suitable technique to study soil granulometry using the Laser Granulometer equipment,[4-6] which operates in a more complex manner to obtain a granulometric curve. In this study, the DLS use proposal was presented as an option to assess the reliability of the physical fractionation method by soil screening and sedimentation, based on the Stokes law, employing ultracentrifugation. The mean diameter and clay polydispersity values of the clays found in each physical fractionation suspension are presented below (Table 2).

We could observe that the clay fraction extraction was well-succeeded, with particle mean diameter ranging between 0.27 and 0.82 μm in the surface layer, and 0.28 and 0.80 μm in the depth layer. These values confirm the efficacy of the clay fractionation process and agree with the literature.[22,29]

The polydispersity index (PDI) refers to the light intensity dispersed through different particle sizes. Values of PDI < 0.1 indicate monodisperse solutions, that is, the particle contained in the solution shows practically the same size. PDI values between 0.1 and 0.7 are

Table 2. Clay fraction mean diameter and polydispersivity (PDI)

Sample	Mean diameter (μm)	PDI	Sample	Mean diameter (μm)	PDI
$C_A(S_1)$	0.27	0.32	$C_P(S_1)$	0.56	0.32
$C_A(S_2)$	0.32	0.47	$C_P(S_2)$	0.28	0.34
$C_A(S_3)$	0.52	0.72	$C_P(S_3)$	0.34	0.57
$C_A(S_4)$	0.47	0.69	$C_P(S_4)$	0.38	0.59
$C_A(S_5)$	0.82	0.87	$C_P(S_5)$	0.52	0.49
$C_A(S_6)$	0.75	0.68	$C_P(S_6)$	0.80	0.73

(C): clay. (S): suspension. (A): soil surface layer. (P): depth layer.

considered moderately polydisperse. Finally, values > 0.7 are highly polydisperse solutions, that is, containing particles with wide bands of size variation.[8,26]

The PDI values in the analyses of clays extracted from the soil surface varied from 0.32 to 0.87, while those extracted from depth ranged between 0.32 and 0.73, revealing that on average, they are classified as moderately disperse, with low aggregate formation. Even the $C_A(S_5)$ sample with 0.87 PDI, which was classified as the sample with different particle sizes, presented a 0.82 μm mean size, which is still within the clay fraction size range.

The graphs below (Figure 2) show the particle size distribution of the 5th and 6th suspensions of the clay fractionation of the surface and depth layers of the soil studied.

The graphs show a bimodal distribution pattern in the 5th suspension and a unimodal pattern in the 6th suspension in both layers. These two distribution patterns were also observed in the remaining suspensions, therefore, we decided to present these two only. The bimodal behavior in the clay DLS analyses might be related to: (1) this fraction high aggregation power, since due to its small size, its specific surface increases significantly, also increasing the clay particle interaction pattern;[30] (2) the shape polydispersity, since clay is a natural material and might contain different types of minerals. Despite these characteristics, when observing all measurements (Table 2), the diameters were not higher than the values set for the clay fraction (0-2 μm).[22]

For this reason, and considering the user-friendliness and speed of the methodology, the technique seems to be a valuable alternative in the experimental confirmation of the clay fraction physical fractionation procedure.

Mid-Infrared Spectroscopy

The infrared spectra of ADFE samples and their granulometric fractions in the soil are presented below (Figure 3). The spectra were divided into two graphs, considering the origin of the soil layer, surface (A) or depth (P), and regarding the sand fraction, the spectra were obtained from a mixture of coarse and fine sand.

The absorption bands in the spectra are represented with numbers and identified considering their functional groups of organic and inorganic components (Table 3). The identification was based on tables and data found in the literature.[9,16]

Regarding the organic components, a wide shoulder is formed in the 3440 cm⁻¹ region for the spectra of the ADFE (A), ADFE (P) and Silt (P) samples. Such shoulder can be ascribed to the free NH (νN-H) stretch. The 1630 cm⁻¹ band might refer to the carboxylate asymmetric stretching (ν_aC=O), aromatic C=C stretching and the stretching of amide groups (amide I band).

The only spectra where this band is absent are those in the Silt (S), Sand (S), and Sand (P) samples. This is mainly due to the low occurrence of humified organic material associated with these fractions.
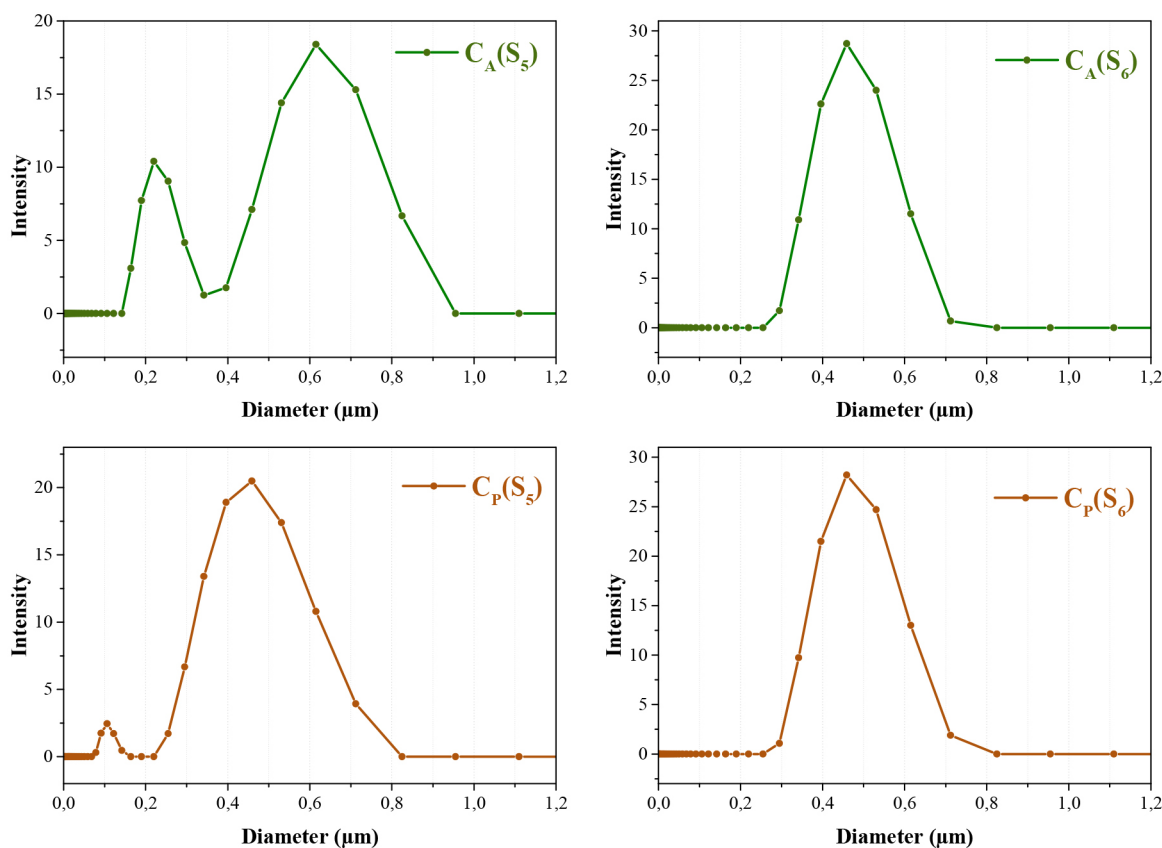
Figure 2. Distribution of clay particle sizes found in the surface and depth layers in the 5th and 6th suspensions of the physical fractionation
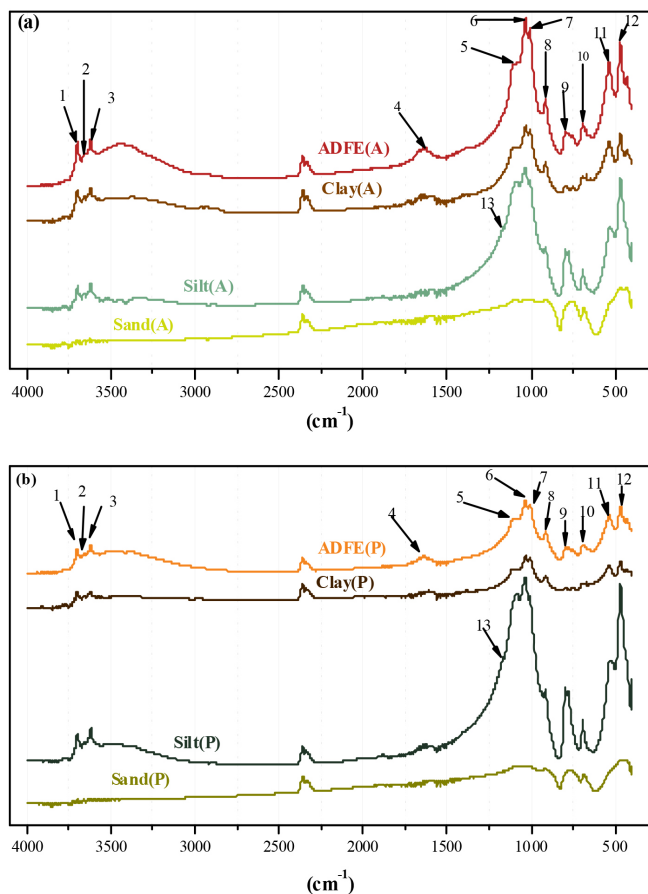
Figure 3. Infrared absorbance spectra of the ADFE samples and their granulometric fractions, obtained from the soil surface (a) and depth (b) layers

The band at 796 cm^{-1} was ascribed to CH angular deformations outside the plane (τC-H). In the spectra of Silt (A) and Silt (P) samples, a small band is observed in the 1165 cm^{-1} region, ascribed to the sulphate stretching (νSO$_4^{-2}$).

When analyzing the inorganic components of the bands found in the MIR absorption spectra, firstly, we observed bands at 3697 cm^{-1} and 3655 cm^{-1} referring to the internal and external OH (νO-H) kaolinite stretching. Also, at 3620 cm^{-1}, an internal OH (νO-H) kaolinite, illite and/or gibbsite stretching was observed. In the 1090 cm^{-1} band, overlapping organic components, the stretching of silicates found in clay and/or quarts was also observed. The region from 1033 cm^{-1} to 536 cm^{-1} presented stretching vibrations, both angular and in the silicate material plane and hydroxyl groups of kaolinite, halloysite, and/or gibbsite. Possible vibrations were also observed at 796 cm^{-1} and 536 cm^{-1} around Al ions of kaolinite, halloysite, and gibbsite.

In the sand fraction spectra, quartz absorption predominated (Figure 3), without any organic or other mineral absorption, which shows the efficacy of this fraction fractionation.

Scanning Electron Microscopy with Field Emission Gun (SEM-FEG)

The SEM-FEG micrography results of the clay fraction are shown below (Figure 4). The clay fraction was seen to present similar morphology in both cases, with particles of varied sizes, irregular surface and some aggregate formation with layered structures.

When analyzing the micrography, in 1 and 2 μm scale (Figure 5), we could verify the predominance of laminar structures, with irregular boundaries and pseudo-hexagonal morphology (red arrows), which might be the kaolinite mineral.[10,11] According to Melo and Wypych,[10] kaolinite formation in soils under the influence of other minerals and/or organic matter and ions that are not part of the mineral structure,

Table 3. Functional groups of organic and inorganic components in the bands identified in the infrared spectra

Peaks	Wave number (cm^{-1})	Functional groups	
		Organic Component	Inorganic Component
1	3697	-	νO-H kaolinite
2	3655	-	νO-H kaolinite
3	3620	-	νO-H kaolinite, νO-H Illite and/or νO-H Gibbsite
4	1630	ν_aC=O, νC=C, amide I band	-
5	1090	νC-O polysaccharide	νSi-O clay minerals and/or νSi-O-Si quartz
6	1033	νC-O polysaccharide	νSi-O-Si Kaolinite, νOH Gibbsite
7	1006	νC-C aromatic and /or νC=S	νSi-O-Si Kaolinite
8	912	-	δOH internal to Kaolinite and/or Gibbsite
9	796	τC-H	νAl Kaolinite, Halloysite and Gibbsite, νSi-O$_2$ (quartz)
10	694	-	νSi-O
11	536	-	νAl, δOH Gibbsite or Kaolinite, δSi-O
12	468	-	δSi-O
13	1165	νSO$_4^{2-}$	-

(ν): stretching. (ν_a): asymmetric stretching. (τ): stretching outside the plane. (δ): angular vibration.
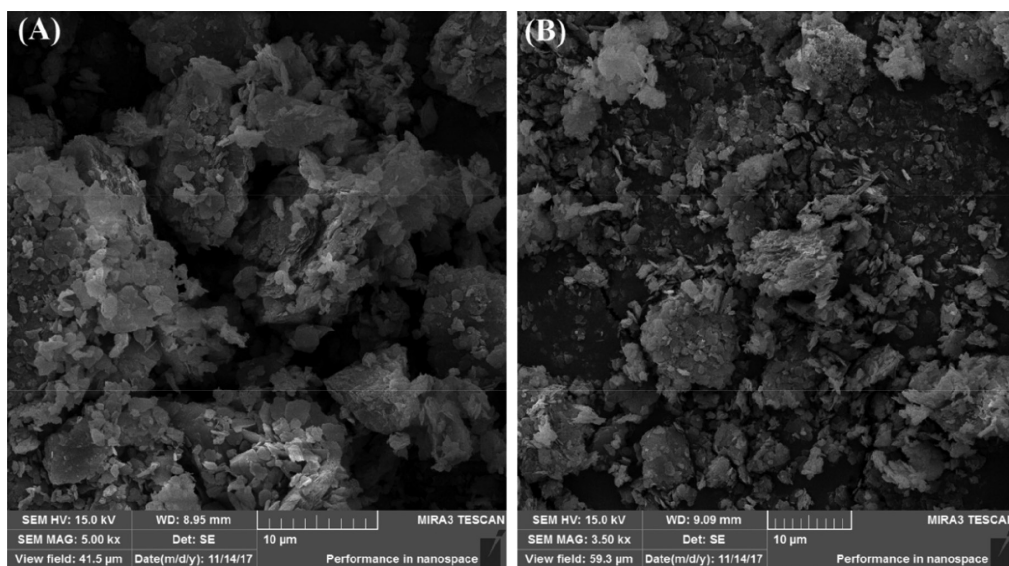
Figure 4. *Micrography of the clay fraction obtained from the soil surface (A) and depth (B), 10 μm scale*

results in the formation of particles with shapes that are not hexagonal. Also, according to D'Acqui *et al.*,[11] who exposed kaolinite to organic residue, they verified that after some time of incubation (30 days), the organic material contributed significantly to the soil aggregation and pore formation, while pure kaolinite, which was also subjected to the same incubation process, did not show the same result. Figure 5(B) shows pore formation, expressed by letter P and, although this is not highlighted in Figure 5(A), this formation is observed in both samples (Figure 4(A)). This might also indicate that this soil fraction contained a significant amount of organic material.

The predominance of the kaolinite mineral was confirmed (Figures 4 and 5), confirming data obtained using the infrared technique, which revealed several peaks characteristic of the absorption in this mineral region. Ferreira,[31] whose study employed X-ray diffraction of the clay fraction obtained from the same soil, also found the presence of kaolinite, quartz, halloysite, muscovite, illite and vermiculite.

The presence of a mineral with filamentous needle-like morphology was also observed (Figure 6). Considering the X-ray diffraction results of the same soil,[31] the MIR spectroscopic analysis

(Figure 3, Table 3) and the morphology of the minerals reported in some studies,[12-14] these images might be illite or halloysite.

According to Lanson *et al.*,[13] particles shaped as thin "strips" or needles, form the illite predominant population. Another study by Lanson *et al.*,[12] which evaluated the morphology of minerals found in sandstones from the Netherlands, reported that with increased depth, the illite mineral showed a harder spear morphology, which can be observed when we compare the micrography of the clay fraction obtained from the soil surface and that of the soil depth (Figure 6).

In a study characterizing clay minerals, Duzgoren-Aydin, Aydin and Malpas[14] evidenced needle-like halloysite. The same study reported that the relative abundance of kaolinite increased when the relative abundance of illite and halloysite decreased. This fact explains, when evaluating the morphology presented in the micrography, the predominance of kaolinite in relation to the other minerals found in lower amounts.

The morphology presented in previous micrography results are related to the minerals that were identified according to their functional groups in the MIR spectra, and also using the X-ray diffractometry analysis by Ferreira,[31] whose study investigated the
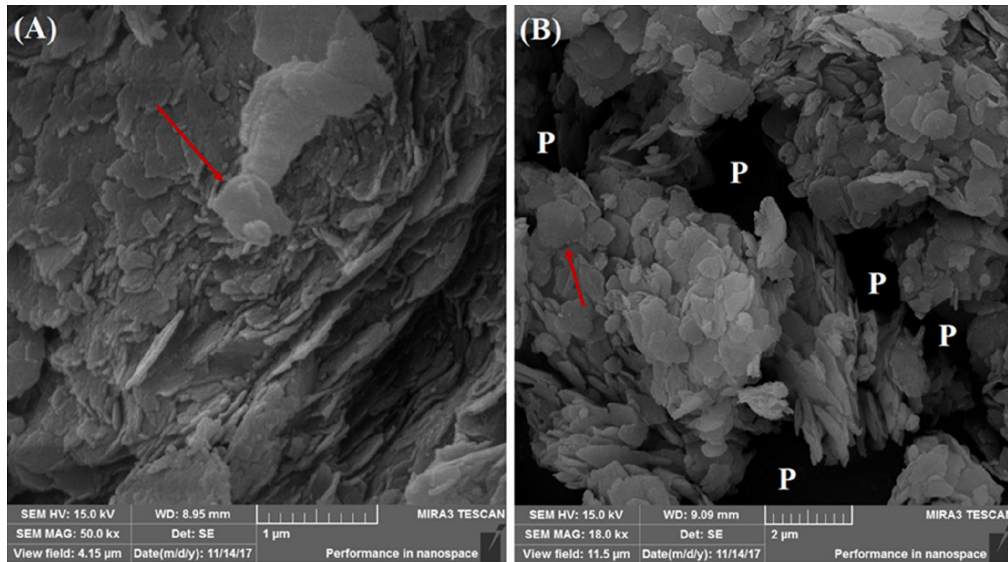
Figure 5. *Micrography of the clay fraction obtained from the soil surface (A) and depth (B), 1 to 2 µm scale. Pores found in the sample (B) are expressed by the letter P. The arrows indicate the kaolinite mineral*
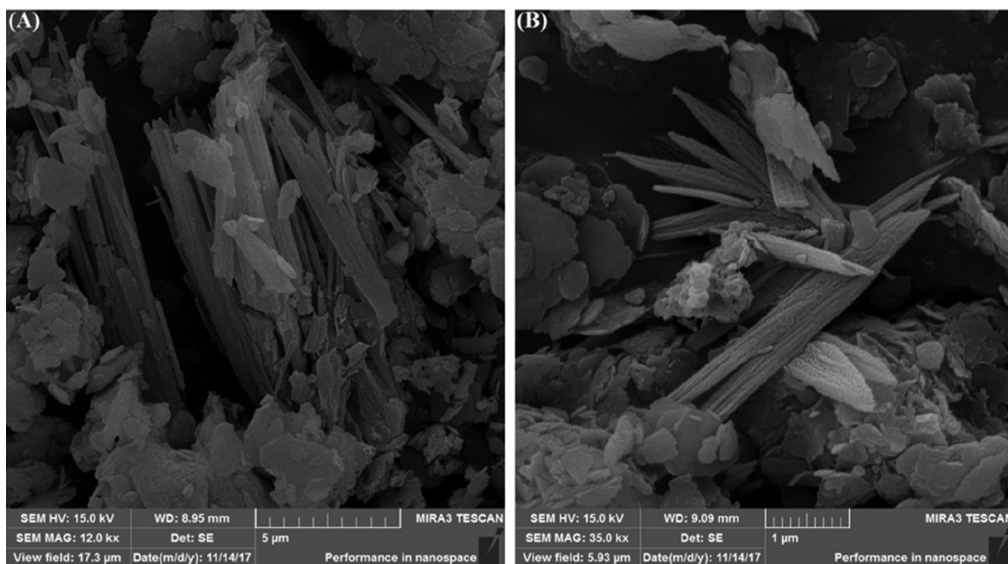
Figure 6. *Micrography of the clay fraction obtained from the soil surface (A) and depth (B), 5 and 1 µm scale*

same soil clay fraction. There are very few works in the literature characterizing the morphology of minerals found in the soil clay fraction without chemical and/or physical treatment, which is the highlight of this study.

CONCLUSION

The quantitative study of granulometric fraction contents obtained using the physical fractionation procedure by soil screening and sedimentation demonstrated that over half of the soil is composed of the clay fraction (≈ 52%). The infrared technique enabled the spectroscopic characterization of organic and inorganic elements found in the soil fractions and in the undisturbed soil (ADFE). Organic attributions prevailed in the clay and silt fractions, and all fractions showed attributions of inorganic groups referring to silicate material. The main minerals found in the granulometric fractions contained kaolinite, halloysite, quartz and gibbsite.

The DLS technique used to evaluate the quality of the clay granulometric fractionation confirmed the absence of particles of other granulometric fractions. The polydispersivity index of the analyses remained in the band of safe values for the mean diameter calculation, which qualifies this technique for the evaluation of the quality of the clay fraction granulometric fractionation.

The SEM-FEG micrography results helped the identification of the minerals' morphology of found in the clay fractions, which was fractioned in its natural form, without chemical or physical treatment. The predominance of laminar structures with irregular boundaries and a pseudo-hexagonal morphology, typical of the kaolinite mineral, was observed. We could also notice the discrete presence of filamentous needle-like morphologies, which could be ascribed to the illite and/or halloysite minerals. Such finding confirms the data obtained with the infrared technique that revealed peaks and bands characteristic of absorption in the region of these minerals.

REFERENCES

1. Brady, C. N.; Weil, R. R. In *Elementos da Natureza e Propriedades dos Solos*, 3ª ed.; Bookman: Porto Alegre, 2013.

2. de Almeida, B. G.; Donagemma, G. K.; Ruiz, H. A.; Braida, J. A.; Viana, J. H. M.; Reichert, J. M. M.; Oliveira, L. B.; Ceddia, M. B.; Wadt, P. S.; Fernandes, R. B. A.; Passos, R. R.; Dechen, S. C. F.; Klein, V. A.; Teixeira, W. G.; *Padronização de Métodos para Análise Granulométrica no Brasil*, 1ª ed.; Embrapa: Rio de Janeiro, 2012. [Link]

3. Prado, G. S.; Campos, J. R.; *Eng. Sanit. Ambiental* **2009**, *14*, 401. [Crossref]

4. Kaszuba, M.; McKnight, D.; Connah, M. T.; McNeil-Watson, F. K.; Nobbmann, U.; *J. Nanoparticle Res.* **2008**, *10*, 823. [Crossref]

5. Pecora, R.; *J. Nanoparticle Res.* **2000**, *2*, 123. [Crossref]

6. Leung, A. B.; Suh, K. I.; Ansari, R. R.; *Appl. Opt.* **2006**, *10*, 2186. [Crossref]

7. Santos, H. G.; *Sistema brasileiro de classificação de Solos*, 3ª ed.; Embrapa: Brasilia, 2013. [Link]

8. Bhattacharjee, S.; *J. Controlled Release* **2016**, *235*, 337. [Crossref]

9. Fabris, J. D.; Viana, J. H. M.; Schaefer, C. E. G. R.; Wypych, F.; Stucki, J. W.; Em *Química e Mineralogia do Solo - Parte I*; Melo, V. F.; Alleoni, F. R. L., eds.; SBCS: Viçosa, 2009, cap. 10.

10. Melo, V. F.; Wypych, F. Em *Química e Mineralogia do Solo - Parte I*; Melo, V. F.; Alleoni, F. R. L., eds.; SBCS: Viçosa, 2009, cap. 7.

11. D'Acqui, L. P.; Daniele, E.; Fornasier, F.; Radaelli, L.; Ristori, G. G.; *Eur. J. Soil Sci.* **1998**, *49*, 579. [Crossref]

12. Lanson, B.; Beaufort, D.; Berger, G.; Baradat, J.; Lacharpagne, J. C.; *J. Sediment. Res.* **1996**, *66*, 501. [Crossref]

13. Lanson, B.; Beaufort, D.; Berber, G.; Bauer, A.; Cassagnabère, A.; Meunier, A.; *Clay Minerals* **2002**, *37*, 1. [Crossref]

14. Duzgoren-Aydin, N. S.; Aydin, A.; Malpas, J.; *Catena* **2002**, *50*, 17. [Crossref]

15. Brinatti, A. M; Mascarenhas, Y. P.; Pereira, V. P.; Partiti, C. S. M.; Macedo, A.; *Sci. Agric. (Piracicaba, Braz.)* **2010**, *67*, 454. [Crossref]

16. Ferraresi, T. M.; Silva, W. T. L.; Martin-Neto, L. Silveira, P. M.; Madari, B. E.; *Rev. Bras. Cienc. Solo* **2012**, *36*, 1769. [Crossref]

17. Dick, D. P.; Santos, J. H. Z.; Ferranti, E. M.; *Rev. Bras. Cienc. Solo* **2003**, *27*, 29. [Crossref]

18. Farmer, V. C.; Palmieri, F. In *Soil Components*, vol. 2, 1st ed.; Gieseking, J. E., ed.; Springer Berlin: Heidelberg, 1975, p. 573.

19. Chukanov, N. V.; Chervonnyi, A. D.; *Infrared Spectroscopy of Minerals and Related Compounds*, 1st ed.; Springer Cham: Switzerland, 2016.

20. Tivet, F.; Sá, J. C. M.; Lal, R.; Milori, D. M. B. P.; Briedis, C.; Letourmy, P.; Pinheiro, L. A.; Borszowskei, P. R.; Hartman, D. C.; *Geoderma* **2013**, *207-208*, 71. [Crossref]

21. Auler, A. C.; Pires, L. F.; Santos, J. A. B.; Caires, E. F.; Borges, J. A. R.; Giarola, N. F. B.; *Soil Use Manage.* **2017**, *33*, 129. [Crossref]

22. Instituto Brasileiro de Geografia e Estatistica - IBGE; *Manual Técnico de Pedologia,* 3ª ed.; IBGE: Rio de Janeiro, 2015.

23. Christensen, B. T. In *Advances in Soil Science*, 1st ed.; Stewart, B. A., ed.; Springer-Verlag: New York, 1992, cap. 1.

24. Schardosin, J.; Dissertação de Mestrado, Universidade Estadual de Ponta Grossa, Brasil, 2018. [Link]

25. Ferreira, T. R.; Pires, L. F.; Brinatti, A. M.; Auler, A. C.; *J. Soils Sediments* **2017**, *18*, 1641. [Crossref]

26. Malvern Instruments; *Zetasizer Nano User Manual*; Malvern Instruments Limited: England, 2013. [Link]

27. Brar, S. K.; Verma, M.; *TrAC, Trends Anal. Chem.* **2011**, *30*, 4. [Crossref]

28. Silva, A. S.; da Silva, I. F.; Bandeira, L. B.; Dias, B. O.; Silva Neto, L. F.; *Cienc. Rural* **2014**, *44*, 1783. [Crossref]

29. Kretzschmar, R.; Holthoff, H.; Sticher, H.; *J. Colloid Interface Sci.* **1998**, *202*, 95. [Crossref]

30. Dufranc, G.; Dechen, S. C. F.; Freitas, S. S.; Camargo, O. A.; *Rev. Bras. Cienc. Solo* **2004**, *28*, 505. [Crossref]

31. Ferreira, T. R.; Tese de Doutorado em Ciências, Universidade Estadual de Ponta Grossa, Brasil, 2018. [Link]